

## Spectral clustering to model deformations for fast multimodal prostate registration

J. Mitra<sup>1,2</sup>, Z. Kato<sup>3</sup>, S. Ghose<sup>1,2</sup>, D. Sidibé<sup>1</sup>, R. Martí<sup>2</sup>, X. Lladó<sup>2</sup>, A. Oliver<sup>2</sup>, J. C. Vilanova<sup>4</sup>, F. Meriaudeau<sup>1</sup>

<sup>1</sup> Univ. de Bourgogne, France, <sup>2</sup> Univ. de Girona, Spain,

<sup>3</sup> Univ. of Szeged, Hungary, <sup>4</sup> Girona Magnetic Resonance Center, Spain

([jhimli.mitra@soumya.ghose/dro-desire.sidibe/fmeriau](mailto:jhimli.mitra@soumya.ghose/dro-desire.sidibe/fmeriau))@u-bourgogne.fr;

[kato@inf.u-szeged.hu](mailto:kato@inf.u-szeged.hu), ([marly/llado/aoliver](mailto:marly/llado/aoliver))@eia.udg.edu \*

### Abstract

*This paper proposes a method to learn deformation parameters off-line for fast multimodal registration of ultrasound and magnetic resonance prostate images during ultrasound guided needle biopsy. The registration method involves spectral clustering of the deformation parameters obtained from a spline-based non-linear diffeomorphism between training magnetic resonance and ultrasound prostate images. The deformation models built from the principal eigen-modes of the clusters are then applied on a test magnetic resonance image to register with the test ultrasound prostate image. The deformation model with the least registration error is finally chosen as the optimal model for deformable registration. The rationale behind modeling deformations is to achieve fast multimodal registration of prostate images while maintaining registration accuracies which is otherwise computationally expensive. The method is validated for 25 patients each with a pair of corresponding magnetic resonance and ultrasound images in a leave-one-out validation framework. The average registration accuracies i.e. Dice similarity coefficient of  $0.927 \pm 0.025$ , 95% Hausdorff distance of  $5.14 \pm 3.67$  mm and target registration error of  $2.44 \pm 1.17$  mm are obtained by our method with a speed-up in computation time by 98% when compared to Mitra et al. [7].*

### 1. Introduction

The appearance of malignant lesions in a Transrectal Ultrasound (TRUS) guided needle biopsy of the

\*Research funded by VALTEC 08-1-0039 of Generalitat de Catalunya, Spanish Sc. & Innovation grant nb. TIN2011-23704, Spain; Conseil Régional de Bourgogne, France; grants CNK80370 of NIH & OTKA; the European Union and the European Regional Development Fund within the project TAMOP-4.2.1/B-09/1/KONV-2010-0005.

prostate is mostly hypoechoic and the accuracy of finding such lesions is typically 43% in sonography. Approximately 25% – 42% of cancer lesions can also be isoechoic and the chance to diagnose hypoechoic malignant lesions from TRUS guided biopsy is  $\leq 57\%$  [3]. Magnetic Resonance (MR) images provide better soft-tissue contrasts, therefore, fusion of pre-biopsy MR images onto interventional TRUS images might increase the overall biopsy accuracy [9].

The prostate of the same patient may exhibit deformations between the TRUS and the MR images. The deformations are caused by the insertion of the endorectal probe during the MR acquisition, bowel or gas inside the rectum and displacement of patient position between the TRUS and MR imaging procedures. However, the deformation is mostly observed as flattening of the part of the prostate adjacent to the rectum. Therefore, in this paper we attempt to model such deformations of the prostate from a set of corresponding MR images co-registered with the TRUS images. The deformable registration of the training set of TRUS and MR images is done using the method of Mitra et al. [7]. However, instead of the geometric approach used in their work to establish point correspondences, we employ the shape-context based method of Belongie et al. [1] and Bhattacharyya distance [2] to set contour point correspondences across the TRUS and the MR prostate images.

The deformable registration in [7] is based on the minimization of the difference in segmented prostate regions where both the TRUS and MR regions are under the influence of a set of polynomial functions. The MR image transformation employs a thin-plate spline (TPS) interpolation. The combination of TPS based interpolation and the set of polynomial functions ensures a smooth diffeomorphic transformation of the MR image at the cost of increased computation time. However, the MR images need to be registered with the TRUS

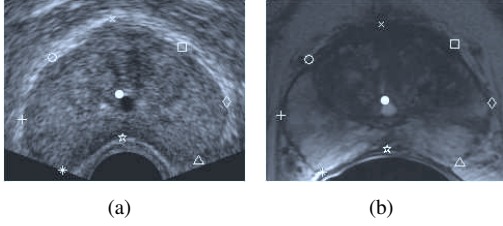


**Figure 1.** Point correspondences example. (a) points in TRUS, (b) point correspondences of (a) in MR.

images in near real time during prostate biopsy. Therefore, to achieve fast registration we propose to model the TPS weight parameters obtained from the diffeomorphic registration of training TRUS-MR images and then apply the modeled parameters to register a new set of TRUS-MR images. Hence, we propose to cluster the deformation vectors using spectral clustering approach and the principal eigen-modes of the deformation vectors of each of these clusters in a Gaussian space form the deformation models. The registration of a test set of TRUS-MR images involves recovering the affine parameters from the established point correspondences and the TPS weight parameters of each of the deformation model are consecutively applied. The model with the least registration error between the TRUS-MR images is chosen as the optimal deformation model.

The remaining paper is organized in the following manner. Section 2 describes the proposed method, Section 3 provides the results related to registration accuracies and the computation time, followed by the conclusions in Section 4.

## 2. The Proposed Method

The proposed method is based on the following components: 1) Point correspondences established on both the TRUS and MR images that are required for both the training and testing phases, 2) the non-linear diffeomorphic framework required for deformation of the training MR images, 3) spectral clustering of TPS weight vectors during the training and 4) linear estimation of deformation parameters applied on the test MR image. The following paragraphs provide descriptions of the afore-mentioned components.

**Point Correspondences:** In this work we use manually segmented prostate shapes for accurate evaluation of our method. However, in future we plan to use some automatic prostate segmentation methods in TRUS and MRI such as proposed in [6]. The segmented prostate contour points are uniformly sampled using fixed Euclidean distance. Let the number of uniformly sampled

points now be represented as  $n$ , then each sample point  $c_i$  may be represented by a shape descriptor that is a  $n - 1$  length vector of log-polar relative distances to points  $c_j$ , where  $i \neq j$ . The shape descriptor is binned into a histogram that is uniform in log-polar space and this histogram is the shape-context representation of a contour point [1] i.e.  $c_i$  is represented by a histogram  $h_i(k, \theta)$  such that

$$h_i(k, \theta) = \# \{c_j, i \neq j : (c_i - c_j) \in \text{bin}(k, \theta)\}, \quad (1)$$

where  $k = \log(\sqrt{(x_{i1} - x_{j1})^2 + (x_{i2} - x_{j2})^2})$  and  $\theta = \tan^{-1} \frac{x_{j2} - x_{i2}}{x_{j1} - x_{i1}}$  of the relative distance  $(c_i - c_j)$ , where,  $c_i = (x_{i1}, x_{i2})$  and  $c_j = (x_{j1}, x_{j2})$ . As suggested by Belongie et al. [1], a total of 5 bins are considered for  $k$  and 12 bins for  $\theta$  that ensures that the histogram is uniform in log-polar space.

In this work we choose the Bhattacharyya distance [2] between the shape-context histograms of two shapes to find the best point correspondence since it is fast to compute. Thus, to match a point  $c_i$  in a shape to a point  $c'_j$  in another shape, the Bhattacharyya coefficients between the shape-context histogram of  $c_i$  and all  $c'_j$  are computed and the  $c'_j$  that maximizes the relation in Eq. (2) is chosen as the corresponding point.

$$\arg \max_{c'_j} \sum_{k=1}^5 \sum_{\theta=1}^{12} \sqrt{\hat{h}_i(k, \theta) \cdot \hat{h}'_j(k, \theta)}, \quad (2)$$

where,  $\hat{h}_i(k, \theta)$  and  $\hat{h}'_j(k, \theta)$  are the normalized shape-context histograms of  $c_i$  and  $c'_j$  respectively.

The smoothness of the transformation between the MR and TRUS images may be guaranteed if the prostate mask centroids are also considered in addition to the contour correspondences. The set of correspondences established will be referred as  $p_i^m$  and  $p_i^f$ , where  $i = 1, 2, \dots, 9$  for the moving and fixed images respectively in the following sections. Fig. 1 shows the 8 contour correspondences and the centroid of the prostate overlaid on the TRUS and MR images.

**Non-linear Diffeomorphism:** Point correspondences established on a pair of training TRUS-MR images are used to align the moving MR image with the fixed TRUS image. Assuming that  $x = [x_1, x_2] \in \mathbb{R}^2$  and  $y = [y_1, y_2] \in \mathbb{R}^2$  are the moving MR and fixed TRUS images respectively, a system of nonlinear equations is constructed as proposed in [4, 7]:

$$\int_{I_f} \omega_t(y) dy = \int_{I_m} \omega_t(\varphi(x)) |J_\varphi(x)| dx. \quad (3)$$

$\varphi(x) = [\varphi_1(x), \varphi_2(x)]$  is the deformation field,  $|J_\varphi(x)|$  is the Jacobian determinant of the transformation at  $x$  of the moving image. Each nonlinear function  $\omega_t(\cdot)$ ,  $t = 1, \dots, l$  generates one equation, yielding a system of  $l$  equations [4]. The transformation  $\varphi(x)$  is a

TPS interpolation of the moving image guided by the set of points established on the same and is given by Eq. (4) where,  $a_{vu}$  are the 6 affine parameters,  $w_{iv}$  are the TPS weight parameters for the control points with  $i = 1, \dots, n$ ,  $v = 1, 2$ ,  $u = 1, 2, 3$ ,  $U(r) = r^2 \log r^2$  is the radial-basis function and  $\|\cdot\|$  is the Euclidean norm.

$$\varphi_v(\mathbf{x}) = a_{v1}x_1 + a_{v2}x_2 + a_{v3} + \sum_{i=1}^n w_{iv}U(\|p_i^m - \mathbf{x}\|),$$

$$\text{s.t. } \sum_{i=1}^n w_{iv} = 0 \quad \text{and} \quad \sum_{i=1}^n p_i^m w_{iv} = 0 \quad (4)$$

The diffeomorphic framework also considers the correspondence localization error across the moving and fixed images and the regularization of the bending energy of the TPS as

$$\frac{1}{n} \sum_{i=1}^n \frac{\|p_i^f - \zeta(p_i^m)\|^2}{\sigma_i^2} + \lambda E_{TPS} = 0, \quad (5)$$

where  $\sigma_i^2$  is the sum of the variances of both the moving and fixed point correspondences,  $E_{TPS} = \Delta^2 \zeta$  with  $\zeta(p_i^m) = p_i^f$ . The adopted set of non-linear functions are the power functions  $\omega_t(x) = x_1^{a_t} x_2^{b_t}$ , with  $(a_t, b_t) \in \langle (0, 0), (1, 0), (0, 1), (1, 1), \dots, (5, 5) \rangle$  which provides sufficiently many equations to obtain a least squares estimate of the  $9 \times 2$  TPS weights and 6 affine parameters. The solution of Eq. (3) with the constraints in Eq. (4) and Eq. (5) is then obtained via the Levenberg-Marquardt algorithm.

**Spectral clustering:** The deformation parameters i.e. the TPS weight parameters obtained for the set of training fixed and moving images are grouped into similar deformation clusters by a spectral clustering approach that determines the number of clusters automatically. Since, the TPS weight parameters are essentially row vectors of length  $9 \times 2$  for x- & y-directions, we firstly compute the resultant direction vector. Then the cosine similarities of  $\mathcal{P} = 9$  resultant deformation vectors of the training set are used to construct a  $\mathcal{P} \times \mathcal{P}$  similarity matrix  $\mathcal{W}$ . The objective is to determine  $k$  disjoint clusters and the algorithm may be defined in the following steps [8]:

- 1) Form the similarity matrix  $\mathcal{W} \in \mathbb{R}^{\mathcal{P} \times \mathcal{P}}$ , i.e.  $\mathcal{W}_{ij} = \frac{W_i \cdot W_j}{\|W_i\| \|W_j\|}$ , where,  $\mathcal{W}_{ii} = 1$ .
- 2) Define the diagonal degree matrix  $D$ , where  $D_{ii}$  is the sum of the row elements of the  $\mathcal{W}_i$ .
- 3) Form normalized Laplacian  $L$  as  $D^{-1/2} \mathcal{W} D^{-1/2}$ .
- 4) Get the first  $k$  eigenvectors of  $L$  to build the matrix  $U \in \mathbb{R}^{\mathcal{P} \times k}$  by stacking the eigenvectors into columns.
- 5) Normalize the matrix  $U$  to  $V$  with unit-length row.
- 6) Treating each row of  $V$  as a point in  $\mathbb{R}^k$ , apply K-means clustering to re-normalized  $V$  matrix.

**Table 1.** Registration accuracies and computation time for different methods. HD and TRE are in (mm) and time is in seconds.

Methods	Mitra et al. [7]	DEF-NL	DEF-L
DSC	0.982±0.004	0.978±0.010	0.927±0.25
HD	1.54±0.46	2.05±1.26	5.14±3.67
TRE	1.90±1.27	1.71±1.23	2.44±1.17
Time	320.79±76.01	106.34±32.45	4.99±3.52

Similar deformation vectors are now grouped into  $k$  disjoint clusters, where  $k$  is the number of largest eigen-vectors comprising 88% of the total variations such that each cluster consists of more than one deformation vector.

**Linear estimation:** Geva et al. [5] showed an off-line linear estimation of basis functions from a deformation space. They performed a PCA of the coefficients of a bivariate B-splines transformation to represent them by their principal eigen-modes. Similarly, given a test moving image we may transform it by the linear estimation of the TPS deformation parameters i.e.  $w_{iv} = \sum_{s=1}^{N_s} a^s b_{iv}^s$ .  $N_s$  is the number of principal axes on which the coefficients are projected after PCA with  $a^s$  and  $b_{iv}^s$  as the respective eigen-value and the eigen-vector. Therefore, the transformation  $\varphi(x)$  of Eq. (3) may be written as

$$\varphi_v(\mathbf{x}) = a_{v1}x_1 + a_{v2}x_2 + a_{v3} + \sum_{i=1}^n \sum_{s=1}^{N_s} a^s b_{iv}^s U(\|p_i^m - \mathbf{x}\|) \quad (6)$$

The eigen-modes of  $k$  deformation clusters with an average of 3 clusters comprise of 95% variation of the principal modes and its Gaussian space of  $-2\sigma, -1\sigma, \dots, +2\sigma$ , with  $\sigma$  as the standard deviation provide 5 deformation models for each cluster. The affine parameters of the TPS transformation are obtained by sum-of-squared differences minimization of the point correspondences established on the test moving and fixed images. Finally to obtain the optimal transformation of the test moving image, the registration error is computed as the percentage of non-overlapping area in prostate foreground and the one with least registration error is considered as the final transformation.

### 3. Experiments and Results

The validation of our new method is done using 25 patients axial mid-gland slices for both the TRUS and MR images with an average size of  $250 \times 200$  pixels with each pixel dimension being  $0.2734 \times 0.2734$  mm. A leave-one-out approach is used where the deformation models are formed from 24 datasets and are applied

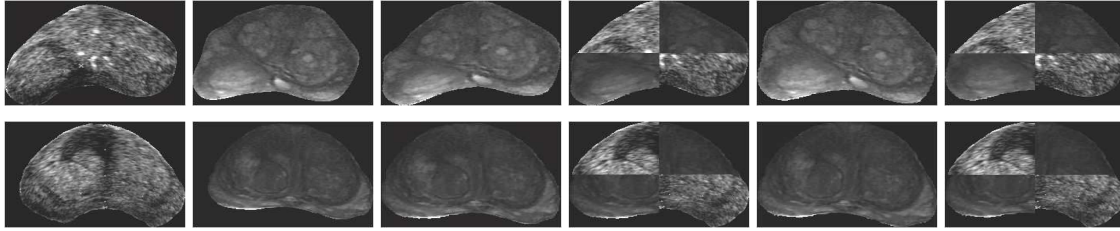


**Figure 2.** Qualitative registration results. The first two columns show the fixed TRUS and the moving MR images respectively. The 3<sup>rd</sup> and the 4<sup>th</sup> columns show the registration results for the proposed method without the deformation learning and the remaining columns show the results with the deformation learning.

to transform the remaining one. The registration accuracy is evaluated in terms of Dice similarity coefficient (DSC) that measures the global overlap of the prostate regions, 95% Hausdorff distance (HD) that measures the contour accuracy and target registration error (TRE) that measures the extent of overlap of the anatomical targets in the transformed MR image and the TRUS image. Table 1 shows the registration accuracies for the method of Mitra et al. [7] with 20 patient datasets, the proposed method with non-linear deformation on improved point correspondences without deformation learning abbreviated as DEF-NL and that with the deformation estimation (DEF-L) i.e. non-linear deformation applied to a set of training TRUS-MR images, spectral clustering to group deformations and thereby applying linearly estimated deformation parameters to transform a test moving MR for 25 datasets in a leave-one-out framework.

It is to be noted in Table 1 that our previous method in [7] using 37 correspondences needs more computation time than our proposed methods DEF-NL and DEF-L with 9 point correspondences. The registration accuracies of DEF-NL are comparable to [7]. The overlap accuracies in terms of DSC and HD for DEF-NL are statistically significantly better with Student's  $t$ -test  $p < 0.0001$  and  $p < 0.001$  respectively than DEF-L. The TRE for DEF-NL is also slightly better than that of DEF-L with a statistical significance of  $p < 0.005$ . Nevertheless, the computation time of DEF-L shows a statistically significant reduction with  $p < 0.0001$  than the remaining methods. Fig. 2 shows the registration results for 2 patients, where it is observed that methods DEF-L and DEF-NL produce similar results. The accuracy of our method DEF-L is qualitatively comparable with that of Xu et al. [9] that demonstrates a near real-time TRUS-MR prostate fusion method with an average registration error of  $2.3 \pm 0.9$  mm but requires 15 s for the registration process. Our method was implemented in MATLAB 2009(b) with 1.66GHz processor and 2GB memory. The method shows a significant speed-up of computation time when the off-line deformation learn-

ing approach is employed while maintaining a clinically significant average target registration error of  $< 3$ mm.

## 4. Conclusions

A method of deformable registration between TRUS and MR prostate images with prior learning of deformation parameters has been proposed. Spectral clustering has been used to group similar deformations from training TRUS-MR images and thereafter the eigen-modes of deformations for each deformation cluster in a Gaussian space have been used to deform a new MR image corresponding to the TRUS image. The method is fast and efficient to transform a moving image with good registration accuracy and may be used during prostate biopsy if programmed on GPU. The accuracy of resulting deformation may be further increased if more patient sets are used to learn the deformation parameters.

## References

- [1] S. Belongie et al. Shape matching and object recognition using shape contexts. *IEEE Trans. on Patt. Anal. & Mach. Intell.*, 24(4):509–522, April 2002.
- [2] A. Bhattacharyya. On a measure of divergence between two statistical populations defined by their probability distribution. *Bulletin of the Calcutta Math. Soc.*, 35:99–110, 1943.
- [3] H. A. Bogers et al. Contrast-enhanced three-dimensional power Doppler angiography of the human prostate: correlation with biopsy outcome. *Urology*, 54(1):97–104, 1999.
- [4] C. Domokos et al. Nonlinear shape registration without correspondences. *IEEE Trans. on Patt. Anal. & Mach. Intell.*, 34(5):943–958, May 2012.
- [5] N. Geva et al. Parametric modeling and linear estimation of elastic deformations. In *Proc. of ICASSP*, pages 1301–1304, 2011.
- [6] S. Ghose et al. Multiple mean models of statistical shapes and probability priors for automatic prostate segmentation. In *MICCAI-PCI*, volume 6963, pages 35–46, September 2011.
- [7] J. Mitra et al. A non-linear diffeomorphic framework for prostate multimodal registration. In *Proc. of DICTA*, pages 31–36, December 2011.
- [8] A. Y. Ng et al. On spectral clustering: Analysis and an algorithm. In *Adv. in Neural Info. Proc. Sys.*, pages 849–856. MIT Press, 2001.
- [9] S. Xu et al. Real-time MRI-TRUS fusion for guidance of targeted prostate biopsies. *Comp. Aid. Surg.*, 13(5):255–264, 2008.